Aerosol Science and Technology, 40:845–860, 2006

ISSN: 0278-6826 print / 1521-7388 online
DOI: 10.1080/02786820600796608

Characteristics of $PM_{2.5}$ Episodes Revealed by Semi-Continuous Measurements at the Baltimore Supersite at Ponca St.

Seung Shik Park,[1,2] Jan Kleissl,[3] David Harrison,[1] Vijayant Kumar,[3] Narayanan P. Nair,[1] Mariana Adam,[3] John Ondov,[1] and Marc Parlange[3]

[1]*Chemistry and Biochemistry, University of Maryland, College Park, Maryland, USA*
[2]*Department of Environmental Engineering, Chonnam National University, 300 Yongbong-dong, Buk-ku, Gwangju 500-757, Republic of Korea*
[3]*Department of Geography and Environmental Engineering, Johns Hopkins University, Baltimore, Maryland, USA*

Highly time-resolved measurements of $PM_{2.5}$, its major constituents, particle size distributions (9 nm to 20 μm), CO, NO/NO_2, and O_3, and meteorological parameters were made from February through November 2002, at the Baltimore Supersite at Ponca St. using commercial and prototype semi-continuous instruments. The average $PM_{2.5}$ mass concentration during the study period was 16.9 μg/m^3 and a total of 29 $PM_{2.5}$ pollution episodes, each in which 24-h averaged $PM_{2.5}$ mass concentrations exceeded 30.0 μg/m^3 for one or more days, were observed. Herein, 6 of the worst episodes are discussed. During these events, $PM_{2.5}$ excursions were often largely due to elevations in the concentration of one or two of the major species. In addition, numerous short-term excursions were observed and were generally attributable to local sources. Those in OC, EC, nitrate, CO, and NO_x levels were often observed in the morning traffic hours, particularly before breakdown of nocturnal inversions. Moreover, fresh accumulation aerosols from local stationary combustion sources were observed on several occasions, as evidenced by elevations in elemental markers when winds were aligned with sources resulting in $PM_{2.5}$ increments of $\sim$17 μg/m^3. Overall, the results described herein show that concentrations of $PM_{2.5}$ and its major constituents vary enormously on time scales ranging from $<$1 hr to several days, thus imposing a more highly complex pattern of pollutant exposure than can be captured by 24-hr integrated methods, alone. The data suggest that control of a limited number of local sources might achieve compliance with daily and annual $PM_{2.5}$ standards.

Received 29 April 2005; accepted 27 April 2006.

Although the research described in this article has been funded wholly by the United States Environmental Protection Agency through grant/cooperative agreement (#BSS R82806301) to University of Maryland, College Park (UMCP), it has not been subjected to the Agency's required peer and policy review and therefore does not necessarily reflect the views of the Agency and no official endorsement should be inferred. Also authors thank personnel from Maryland Department of the Environment (MDE) for providing criteria gas data and for other instrument support.

Address correspondence to John Ondov, Chemistry and Biochemistry, University of Maryland, College Park, MD 20742, USA. E-mail: jondov@wam.umd.edu

1. INTRODUCTION

Atmospheric aerosol is a complex mixture of particles from a large number of discrete sources (Ondov and Wexler 1998). Its size distribution, composition, morphology, and source strengths can vary significantly with meteorology, location, and time. This is especially true for urban atmospheres wherein emissions from concentrated industrial and dispersed sources lead to urban pollutant excesses above rural background concentrations. Changes in chemical composition of particles also lead to changes in the refractive index, therefore affecting visibility and radiation balance (Appel et al. 1985; IPCC 1996; NRC 1996). Information on spatial and temporal variability is of special interest as it can be exploited to determine sources of PM, and may be needed to properly assess acute health effects (Pope 2000). For example, recent epidemiological evidence suggests that short-term transient $PM_{2.5}$ events can trigger the onset of myocardial infarction within a few hours (Peters et al. 2001). For these reasons, EPA has embraced the development of semi-continuous monitors for near real-time analysis of PM and its constituents (Lim et al. 2003; Solomon et al. 2003; Weber et al. 2003a and 2003b) and funded their deployment at seven U.S. "supersites." One of the key features in using real-time instruments is the possibility of differentiating diurnal patterns of major $PM_{2.5}$ chemical species, i.e., sulfate, nitrate, and carbonaceous particles, which make up substantial fractions of urban PM mass. For example, results from a limited, but growing number of studies (e.g., Watson and Chow 2000) show that particulate nitrate and carbonaceous species in eastern United States generally peak in the morning rush hours or sometimes in evening hours (Lim and Turpin 2002; Weber et al. 2003a; Park et al. 2004a, 2004b), sulfate, in

contrast, peaks on summertime afternoons when ozone levels are highly elevated (Weber et al. 2003b), whereas peaks in nitrate concentrations in the western United States frequently occur in the afternoon hours (Stolzenburg and Hering 2000).

Previous observations suggest that short-term, i.e., transient, events are primarily driven by one or two major chemical components of $PM_{2.5}$ (Weber et al. 2003b) and, thus, are derived from a limited number of generic sources. Such transients are often induced by near-by sources. The coincidence of PM excursions with excursions of primary tracer species and metrics of source strengths (e.g., NO, CO, and traffic counts for motor vehicles; Se for coal combustion aerosol; ozone for secondary sulfate and organic matter, i.e., OM) provides further information on its source and source proximity. Furthermore, aged aerosol tends to contain larger particles than fresh primary aerosol from local sources (Dodd et al. 1990; Ondov and Wexler 1998, and references therein), hence size distribution data also reveal important information on source proximity. Moreover, a great deal of additional information on the sources of aerosol particles can be derived from the primary pollutants (e.g., Gordon 1988). Short-term data for these species have been correlated with wind direction to identify (Kidwell and Ondov 2001; Kidwell and Ondov 2004) and apportion (Rheingrover and Gordon 1988; Park et al. 2004) contributions of single sources. The origin of secondary aerosol can be inferred from meteorological conditions and air mass transport vectors.

The Baltimore Supersite study was designed to develop an extended set of highly time, size, and compositionally-resolved PM data for use in apportioning sources, elucidating their health effects, and ultimately to provide information for development of State Implementation Plans. During this study, concentrations of $PM_{2.5}$, major constituents (sulfate, OC, nitrate, and EC), and its size distribution (9 nm to 19 μm) were measured at frequencies ranging from 5 min to 1 hour for a period of 9.5 months in 2002 at Ponca St. in East Baltimore City. The discussion of air pollution is frequently framed in terms of episodes in which increases in health effects (historically "killer smogs") or levels exceeding air quality standards are observed. Herein, we characterize the temporal behavior of $PM_{2.5}$ and its principle constituents for six of thirteen episodes of PM excursion observed during the study period, and provide a descriptive analysis encompassing the PM data, underlying meteorology, and transport. Our intent is to provide a useful summary and a framework for receptor modeling and further exploration of the data.

2. EXPERIMENTAL

2.1. Site Description

Highly time-resolved measurements of $PM_{2.5}$, nitrate, sulfate, elemental and organic carbon (EC and OC), and particle size distributions were made at intervals ranging from 5 minutes to 1 hour from February 14 through the end of November 2002 using commercial and prototype semi-continuous instruments. The Ponca St. site (latitude 39.29°N, longitude 76.55°W, ASL 40 m) is located in an urban residential area, due east of downtown Baltimore and north of the heavily industrial south Baltimore area, so that emissions from these areas could be resolved during typical westerly and southerly flow regimes. Ponca St. is adjacent to I895 (the Harbor tunnel throughway) immediately to the east of the site. Moreover, the site is located at a point, where I895 turns northeast at an angle of $\sim$30°, such that I895 becomes a 7.0 km line source for traffic emissions when winds come from this direction. At that distance I895 converges with I95 and the Baltimore Beltway, which further increases the density of traffic emissions from that angle. It also lies within 90 m of the MTA bus maintenance facility immediately to the southwest. Baltimore is a major Mid-Atlantic transport corridor. More than 300,000 motor vehicles including >30,000 diesel trucks pass through the area's 3 main toll facilities each day. East-end tunnel toll facilities lie along angles of 190 and 200°. The traffic on MD 395 that feeds downtown Baltimore from I95, is typically 360,000 vehicles/day. Below, we briefly describe measurement instruments used at the Baltimore Ponca St. site. Eastern Standard Time (EST) is used throughout.

2.2. Measurements

2.2.1. 24-hour $PM_{2.5}$ Mass and Speciation Measurements

In addition to semi-continuous monitors described below, 24-h samples for routine speciation parameters (sulfate, nitrate, EC, OC, and elemental composition by XRF) and $PM_{2.5}$ mass determinations were collected with a SASS^{TM} ambient chemical speciation (Met One Instruments, Inc., Grants Pass Oregon) and Federal Reference Method (FRM, Andersen RASS100) samplers.

2.2.2. Semi-Continuous $PM_{2.5}$ Mass Measurements

Total $PM_{2.5}$ mass concentration was determined continuously every 30 minutes with a tapered element oscillating microbalance (TEOM R&P 1400a, at 30°, with a naphion dryer) from March 27 to May 23, and from July 4 to November 30, 2002. Integrated 24-h averages of 30-minute TEOM $PM_{2.5}$ data were compared with those from 24-h integrated MetOne speciation $PM_{2.5}$ and FRM $PM_{2.5}$ monitors, for which the regression relationships; $PM_{2.5}$TEOM ($\mu g/m^3$) = (1.075 $\pm$ 0.022) MetOne $PM_{2.5}$ ($\mu g/m^3$) + ($-$2.315 $\pm$ 0.517), R^2 = 0.954 and $PM_{2.5}$ TEOM ($\mu g/m^3$) = (1.031 $\pm$ 0.042) FRM $PM_{2.5}$ ($\mu g/m^3$)+ (0.314 $\pm$ 0.797) and R^2 = 0.882, suggest that our continuous TEOM measurements provide excellent agreement with 24-h integrated speciation and FRM $PM_{2.5}$ mass. Therefore, no adjustments were made to reconcile FRM and TEOM derived mass concentrations.

2.2.3. Semi-Continuous Nitrate Measurements

Particulate nitrate was measured every 10 minute using an R&P 8400N monitor (Rupprecht & Patashnick Co., Inc, Albany, NY), wherein particles are analyzed, in place, after flash vaporization. Details have been described by Harrison et al. (2004).

The nitrate data were corrected for span-gas calibrations (audit correction factors), Rcell pressure deviations, and conversion efficiency using pipetted KNO_3 standards. Then, 24-h nitrate averages were correlated against 24-h integrated measurements derived from ion chromatography of the speciation monitor samples, and then corrected using a slope and intercept to adjust the R&P to the speciation data. Harrison et al. (2004) reported that nitrate concentrations were typically ~30% lower in R&P nitrate monitor than MetOne nitrate measurements in the Baltimore aerosol.

2.2.4. *Sulfate Measurements*

Particulate sulfate was measured every 20 minute using a prototype Harvard sulfate monitor. In this instrument, sample air was aspirated at 0.55 L min^{-1}, denuded of ambient SO_2 *via* a sodium carbonate coated annular glass denuder prior to reduction of particulate sulfate to SO_2 in a 1.8 m 1/8″ o.d. resistively heated stainless steel tube, and detected with a commercial SO_2 analyzer (Model 43C trace level, Thermo Electron Instruments, Franklin, MA). After May 16, a carbon monolith denuder was installed to minimize the NO_x interference. To remove positive interference from other gases, HEPA filtered ambient air is measured (for 6 min) before and after each 14 minute sampling interval. Sulfate concentrations were corrected for span gas audit factors, dynamic blank corrections, and nitrate interference. Then, 24-h averages were compared with 24-h integrated speciation data to derive the conversion efficiency of the sulfate monitor. A detailed description of the monitor, data collection, reduction, and quality assurance measures can be found elsewhere (Harrison et al. 2006). Briefly apparent efficiency of our prototype Harvard sulfate monitor varied somewhat less within each month than it did from month-to-month. Therefore, monthly efficiency correction factors were used to correct the semi-continuous sulfate data.

2.2.5. *Organic and Elemental Carbon Measurements*

$PM_{2.5}$ organic and elemental carbon (OC and EC) concentrations were measured hourly with an in-situ thermal-optical transmittance carbon analyzer (Sunset Laboratory, Beaverton, OR). Data corrections including adjusting sampling volumes to ambient temperature and pressure, and dynamic field blank for OC and EC measurements were applied and their 24-h averages were regressed against 24-h integrated OC and EC data derived from speciation monitor data after analysis by RTI (Research Triangle Institute, NC). The resulting semi-continuous data were then adjusted to agree with speciation OC and EC results using the regression coefficients and offsets derived after removing obvious outliers, as described by Park et al. (2004a), Semi-continuous EC and OC (s-EC and s-OC) measurements were significantly less than the 24-h integrated RTI values (for semi-continuous versus 24-h data, regression slopes and intercepts were: 1.13 and +0.44 μg EC/m^3; and 1.28 and +0.71 μg OC/m^3, respectively).

2.2.6. *Particle Size Distributions*

Particle size distributions from 9.8 nm to 457 nm and from 484 nm to 20.5 μm were respectively measured every 5-minute with a Scanning Mobility Particle Sizer (SMPS, TSI Inc., model 3080) and an Aerodynamic Particle Sizer (APS, TSI Inc., model 3321). The instruments were operated without dryers or humidifiers, but were located in the air-sampling trailer and, thus, at an effective temperature of about 20°C. Particle number distributions are used to characterize $PM_{2.5}$ pollution episodes identified below.

2.2.7. *Meteorological Data*

Temperature, relative humidity (RH), wind speed (ws) and direction (wdir), pressure, precipitation, and solar radiation were recorded on 5-minute intervals by sensors placed on a 10-m tower. Also stream-wise, cross-stream, and vertical velocities (u, v, w) were measured with a 3-d sonic anemometer (CSAT3, Campbell-Scientific), and used to derive friction velocity, Monin-Obukhov length, and sensible heat flux. Additionally, the Johns Hopkins University (JHU) elastic backscatter lidar system (JHU 2000) was used to measure particle scattering at 30-minute intervals. The lidar system was operated at 1.06 μm in upward pointing mode, with a time resolution of five seconds and a range resolution of three meters.

To aid in interpretation of synoptic conditions during the pollution events observed in our study, radiosonde data (NOAA Forecast Systems Laboratory, FSL, http://www.fsl.noaa.gov), MODIS image data (http://modis.gsfc.nasa.gov), composite surface data (provided by Unisys weather, http://weather.unisys.com/surface), and visibility data at Baltimore-Washington International Airport (BWI) (http://www.wunderground.com/history/airport/KBWI/2002) were acquired. In addition, 72-h air mass backward trajectories (Hysplit model, Draxler and Rolph 2003) were computed for periods of interest for an initial height of 500 m. Numerous plots obtained from the above websites and detailed descriptions of the meteorology during the pollution events can be found at http://www.jhu.edu/~dogee/mbp/supersite2001/metsummary.

All data generated from each of the instruments were loaded into Baltimore Supersite (BSS) relational database and flagged on the basis of instrument parameter conditions and operator logs. Project data are available at http://www.supersitesdata.umd.edu.

3. RESULTS AND DISCUSSION

3.1. TEOM $PM_{2.5}$ Mass Concentrations and Identification of $PM_{2.5}$ Episodes

The average of the 30-min $PM_{2.5}$ mass concentrations for the 9.5 month study period was 16.9 ± 13.0 $\mu g/m^3$ and the maximum was 198 $\mu g/m^3$; 24-h averages of $PM_{2.5}$ ranged from 3.5–85.6 $\mu g/m^3$. The US EPA National Ambient Air Quality Standard (NAAQS) of 65.0 $\mu g/m^3$ $PM_{2.5}$ was clearly exceeded only during the Canadian Boreal forest fires. An interesting

feature revealed by the high time-resolution measurements is the presence of short-term (3-h) events, such as those shown in Figure 1 for $PM_{2.5}$ mass, sulfate, and other species. It is apparent that $PM_{2.5}$ mass was highly variable on a time scale of 1 h and that the use of 24-h average largely masks this variability. For example, hourly averaged $PM_{2.5}$ mass concentrations on July 7 and November 20 reached 180 and 86.6 $\mu g/m^3$, respectively, i.e., approximately 2–3 times greater than the 24-h averages (respectively 85.6 and 32.0 $\mu g/m^3$) for these days.

Herein, we identify $PM_{2.5}$ episodes as those periods for which daily average TEOM $PM_{2.5}$ mass exceeded the 9.5-month average (16.9 ± 13.0 $\mu g/m^3$) by one standard deviation (i.e., those ≥ 30.0 $\mu g/m^3$). Based on this criterion, 13 $PM_{2.5}$ episodes were identified. These included five sulfate haze events and six events characterized by high OC, EC, CO, and NO_x during morning (or evening) traffic periods associated with unfavorable dispersion conditions. Six of the 13 episodes, designated A through F, are discussed below. Temporal profiles of $PM_{2.5}$ concentrations and dominant chemical constituents (i.e., sulfate, OC, EC, or nitrate) during each of these are shown in Figure 1, along with those of the relevant meteorological parameters. Likewise, those for O_3, NO_x, and CO are also shown. Particle size distributions are shown in Figure 2. These include daily averaged distributions and averages for specific hourly periods during each of the six PM episodes. The remaining episodes were either similar or encompassed periods of incomplete data collection and are not shown. Descriptive information and statistics for the various parameters during each episode are given in Tables 1 and 2.

3.2. Mass Balance Closure

Herein, mass balance closure is assessed by comparing $PM_{2.5}$ TEOM mass to reconstructed $PM_{2.5}$ mass on an hourly-basis. Ammonium, a principle cation, was not measured in this study. Therefore, reconstructed $PM_{2.5}$ mass concentrations were calculated on the basis of nitrate NH_4NO_3, and sulfate as $(NH_4)_2SO_4$. Also organic matter was estimated from OC by applying a factor to account for oxygen and hydrogen as suggested by Turpin and Lim (2001). Herein factors in the range 1.2–1.8 were applied as follows: 1.8, in June, July, and August, when aerosol mass contains more secondary organic components associated with increased photochemical activity; and 1.4, for the other months except episode F. For episode F, we used a value of 1.2 (the ratio of mass:C mass in normal hydrocarbons with more than 2 C atoms) because the weather was cool, ozone levels were low, and better mass closure was achieved.

Average, minimum, and maximum concentrations for reconstructed $PM_{2.5}$, EC, nitrate (expressed as "NH_4NO_3"), sulfate (expressed as "$(NH_4)_2SO_4$"), and OC (expressed as "organic matter (OM)") concentrations are listed for each of the episodes in Table 2 along with those for TEOM $PM_{2.5}$. TEOM and reconstructed $PM_{2.5}$ mass ($PM_{2.5R}$) for five (B-F; TEOM data are not available for episode A) of the six PM episodes are compared on an hourly basis in Figure 3. As shown, all constituents were highly correlated with measured $PM_{2.5}$ concentrations. Correlation coefficients (R^2) of 0.924–0.995 were large, and regression slopes ranged from 0.79–0.95, indicating some underestimation of the reconstructed mass. Some of the missing mass is water, and some is attributable to suspended dust (e.g., soil). To estimate suspended dust contributions to $PM_{2.5}$ mass for the identified episodes, we used the equation (Soil ($\mu g/m^3$) = 2.20(Al) + 2.49(Si) + 1.63(Ca) + 2.42(Fe) + 1.94(Ti)) reported by Malm et al. (1996) and composition of crustal species derived from the 24-h integrated MetOne speciation samples by XRF. Estimated soil contributions ranged from 1.4 (episode B) to 4.1% (episode F). Thus soil components appeared to be minimal and much of the remaining mass, i.e., 5 to 21%, must be attributed to either error in the assumptions used in mass reconstruction and/or aerosol water content. We note, however, that regression equations for reconstructed- versus TEOM $PM_{2.5}$-mass had significant intercepts (about 4 to 5 $\mu g/m^3$) for episodes D, E, and F. These occurred when there were substantial concentrations during the early morning traffic period; hence, it might be that a smaller OM-to-OC ratio should have been applied. Or, perhaps that more of the sulfate was in the form of NH_4HSO_4.

TABLE 1
Characteritics of six $PM_{2.5}$ episodes identified at the Baltimore supersite in 2002

			Ozone (ppb)[1]		Ambient temp (°C)		Relative humidity (%)		Maxima NO_x and CO, ppb	
Episode	Date	Type	Avg.	Range	Avg.	Range	Avg.	Range	NO_x	CO
A	June 24–25	Regional Haze	84	26–132	29.8	23.7–35.4	57	32–77	110	800
B	July 6–8	Canadian Smoke	—	—	25.6	19.7–33.8	45	28–70	155	1600
C	July 18–19	Regional Haze	70	14–91	29	23.2–34.0	58	38–81	130	800
D	Aug. 12–14	Reg Haze + Local Traffic	76	22–122	29.2	21.6–35.6	54	35–79	300	1800
E	Oct. 2–5	Regional Haze	35	1–57	24.8	17.5–30.4	69	36–91	180	1300
F	Nov. 20–21	Local Traffic	2	0–6	8.4	3.1–14.5	83	48–98	780	2800

[1]Ozone mixing ratios represent measurements made between 10:00 and 20:00 hours.

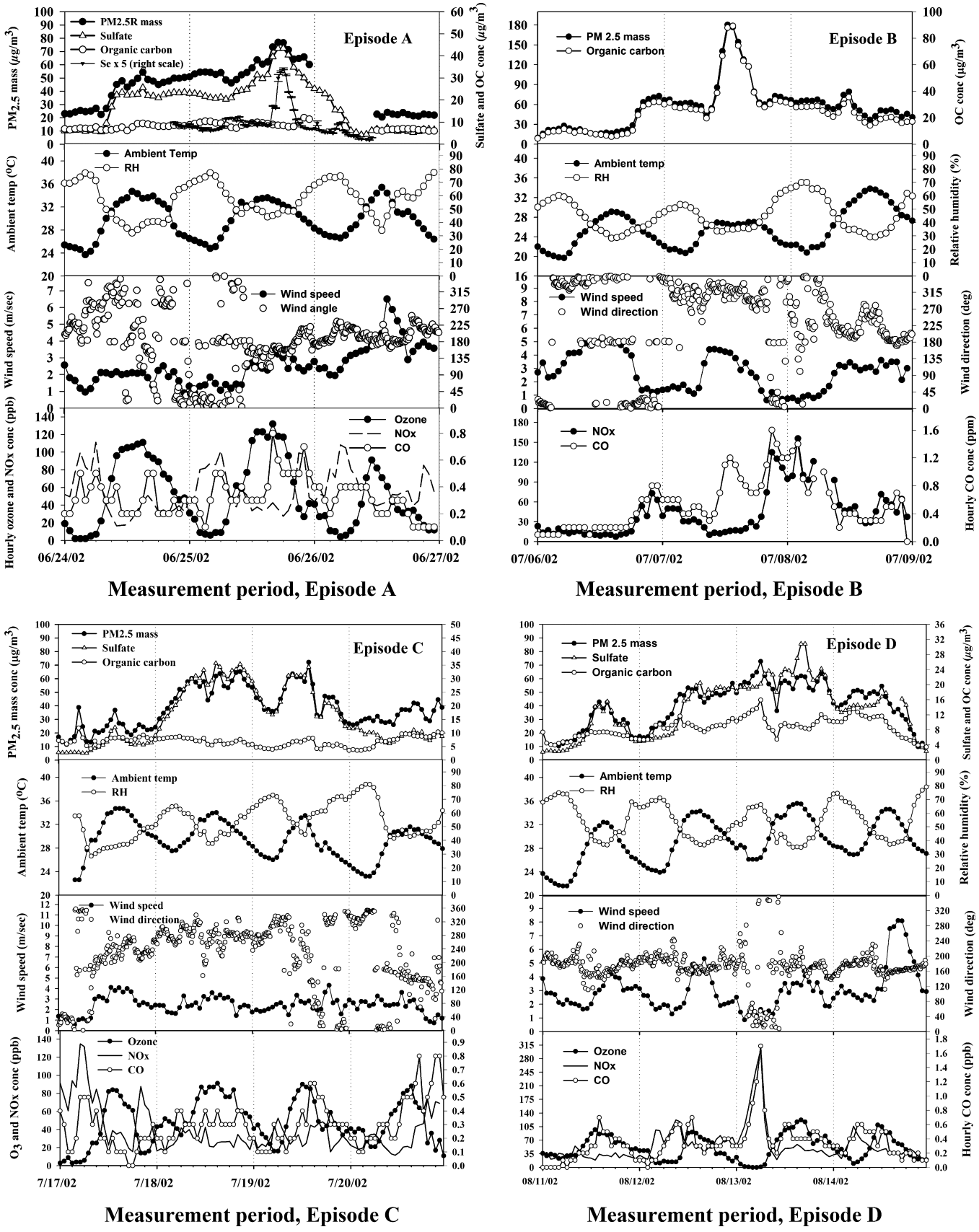

FIG. 1. Temporal variations of $PM_{2.5}$ mass, major chemical species, ambient temperature, relative humidity, wind speed and direction, O_3 NO_x, and CO for PM pollution, A–D.

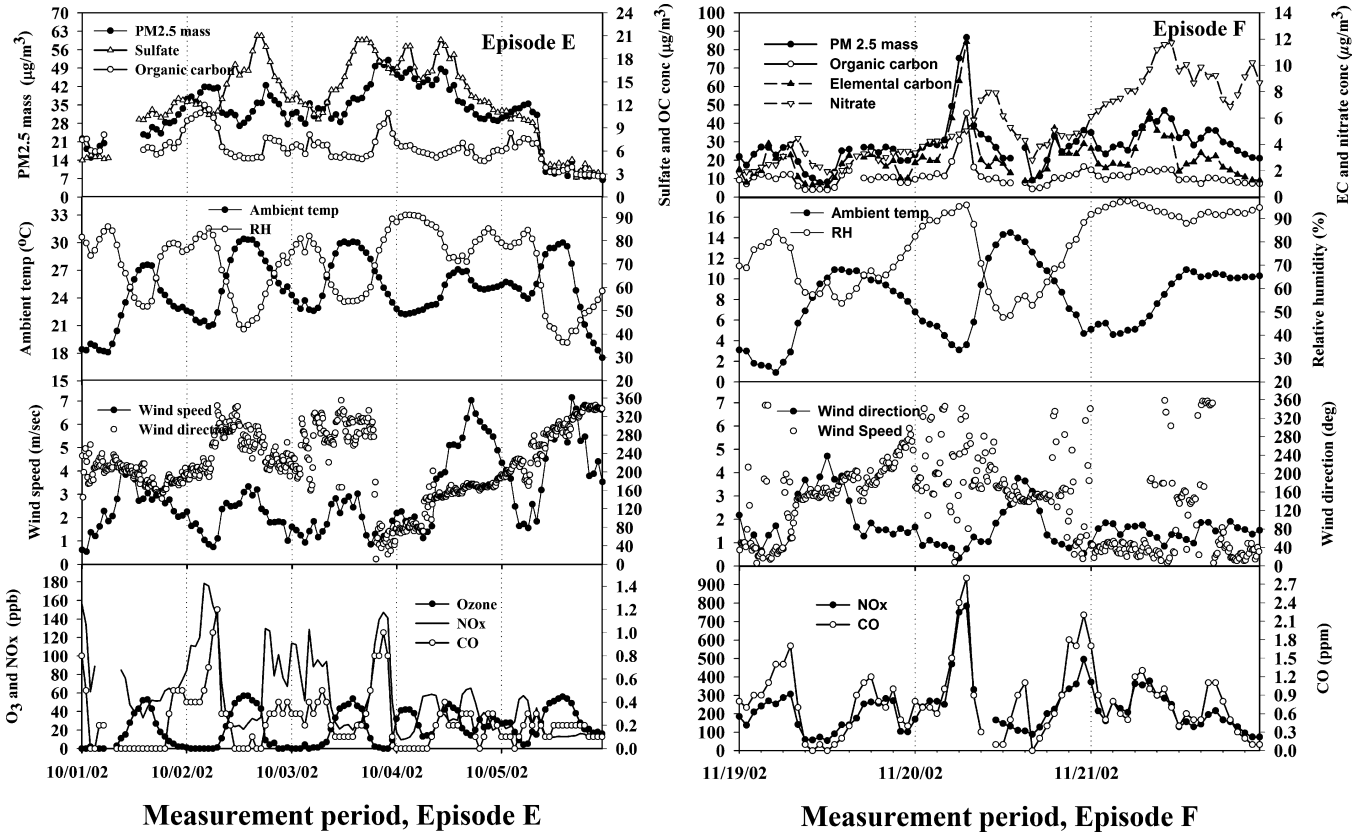

FIG. 1. Temporal variations of $PM_{2.5}$ mass, major chemical species, ambient temperature, relative humidity, wind speed and direction, O_3 NO_x, and CO for PM episodes, E and F.

3.3. Description of PM Pollution Episodes

3.3.1. Episode A (Tuesday–Wednesday, June 24–25, 2002)

Episode A spanned a two-day period during which $PM_{2.5R}$ increased from background levels of 22 $\mu g/m^3$ to a maximum of 78 $\mu g/m^3$. On the worst day, i.e., June 25th, the 24-h average $PM_{2.5R}$ was 59 $\mu g/m^3$, which on the basis of regression equations for Episodes C and D (Figure 3), corresponds to 63 to 65 $\mu g/m^3$, as would have been measured by the TEOM (or FRM) monitor. This is near, but less than the 24-hr $PM_{2.5}$ standard of 65 $\mu g/m^3$. As indicated in Figure 1, the episode was clearly characterized by elevated sulfate and afternoon ozone concentrations (110 and 132 ppb on the 24th and 25th). As shown in Table 2, $(NH_4)_2SO_4$ and OM (expressed as 1.8∗OC; and 65 and 29% of $PM_{2.5}$, respectively) are estimated to have comprised from 86 to 98% of the $PM_{2.5R}$ mass during the episode, whereas EC and NH_4NO_3 constituted only minor (1.0–5.3%, and 1.1–9.9%, respectively) percentages.

$PM_{2.5}$ mass was strongly correlated with sulfate and APS particle number concentrations (R^2 of 0.969 and 0.833), suggesting that the measured particles (i.e., diameters >0.486 μm) were highly processed (see Figure 1 and Table 3). APS concentrations were only moderately correlated with OC concentrations (R^2 of 0.605) which suggest that OC has a greater fine-particle contribution than sulfate.

The episode began at 7:00 PM on June 24 after a stationary front developed over New Jersey resulting in stagnation over the mid-Atlantic region with local wind speeds ranging from 1 to 2.2 m/s. It ended 48 h later as wind speeds increased from a morning low of 1.5 m/s to a high of 6 m/s with the passage of a cold front at 3:00 PM on the 26th. During the first 24 hours strong capping of the boundary layer was coincident with recirculation of hot (daily afternoon maxima 33 to 35°C), dry (RH between 32 and 77%) air within the local region encompassing Maryland, West Virginia, northern Virginia, and southern Pennsylvania (Figure 4). As shown in Figures 1 and 4, $PM_{2.5R}$ and sulfate concentrations were moderately low (respectively 23 and 6 $\mu g/m^3$) early on the 24th, reflecting air originating off the Atlantic coast 3 days earlier and arriving at Baltimore from the southwest. These "background" levels continued until approximately 7:00 AM on the 24th when concentrations increased rapidly (to 46 and 23 $\mu g/m^3$, respectively) and remained near these levels until the end of the capping inversion on the 25th. Between 9:00 AM and 12:00 noon on the 25th, concentrations rose further (to approximately 60 and 30 $\mu g/m^3$), coincident with arrival of air which had been stagnant over the Ohio Valley 3 days earlier (Figure 4). This occurred following the break up of the capping inversion, after which surface wind speeds increased to between 2 and 3 m/s.

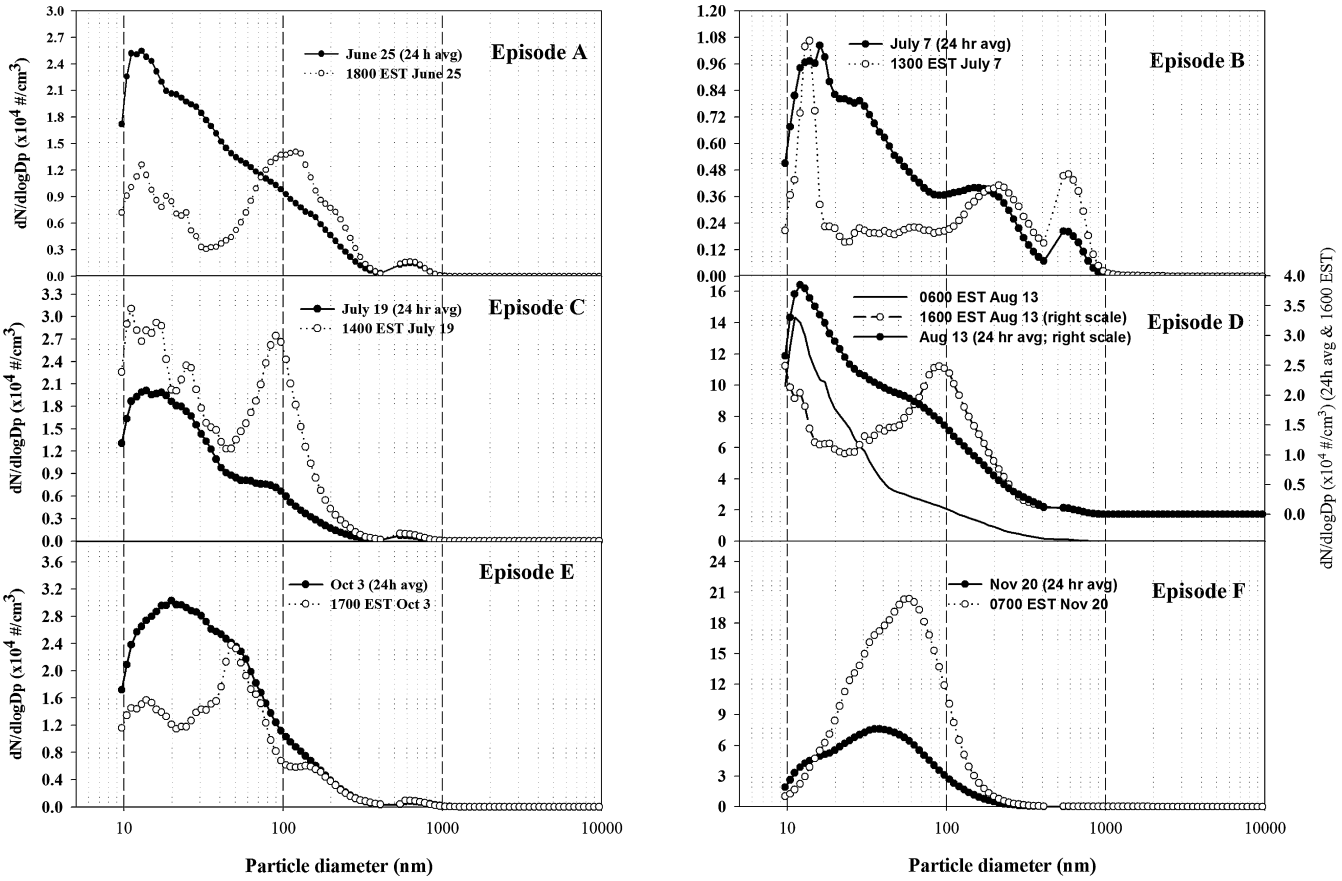

FIG. 2. 24-h average and selected 5-min average sizes pectra determined during episodes A–F.

Superimposed on this later period, are yet further increases in $PM_{2.5}$ and sulfate concentrations for about 5 hours, the onset of which occurred about 3 hours after the wind shifted to 170°, at which angle lies a large coal- and smaller oil-fired power plant at a distance of 15 km. As shown in Figure 1, the maximum sulfate concentration (43.5 μg/m^3) occurred between 3:00 and 6:00 PM, i.e., precisely when selenium (Figure 1), a marker of coal combustion aerosol, and Zn, Cd, and Pb, suggest the influence of local power-plant and incinerator plumes. However, a larger number of industrial sources in South Baltimore may have contributed to the observed increments in aerosol mass and sulfate at this time. The particle size spectrum (Figure 2) at 6:00 PM June 25, i.e., the time of the largest sulfate concentration observed in this episode, show a distinct peak at 0.12 μm containing substantially more particles (peak interval concentration14,000 cm^{-3}/dlogDp) than the period immediately before or after the period of plume influence. This peak is consistent with fresh accumulation aerosol in plumes of nearby power plants and incinerators (Ondov and Wexler 1998). (Note that a second peak, i.e., at 0.63 μm, likely contains secondary sulfate, nitrate, and organic carbon, which on the basis of modal diameter we attribute to aged aerosol.)

On the basis of the sulfate time series data (43.5 μg/m^3 during; 32 μg/m^3 before the period of local influence), the plumes of local stationary sources induced an incremental increase in the ambient sulfate concentration of about 11 μg/m^3; and similarly derived, an increment of 17 μg/m^3 (77−60 μg/m^3) in $PM_{2.5R}$. By integration, this local contribution is approximately 5% of the $PM_{2.5R}$ observed during the excursion period after the capping inversion ended. We argue that concentrations observed during the first 25 hours of the episode were induced by pollutants trapped by stagnation in the "local region," constituting Maryland, northern *West Virginia*, northern Virginia, southern Pennsylvania, and western Delaware, and thus reflect sources emitting therein. Likewise integrating suggests that these might have contributed up to 48% of the excess over background during the entire 2-day episode.

A peak at 0.013 μm (13,000 cm^{-3}/dlogDp) is also contained in the particle size spectra for 6:00 PM on June 25 (Figure 2). This likely reflects, in part, fresh motor vehicle exhaust emissions from I895/I95, which were also immediately upwind at this time. Zhu et al. (2002) observed modes at 12.6 nm 30 m downwind of a Los Angeles freeway, i.e., in good agreement with our value of 13 nm.

OM, Nitrate, and EC. OC concentrations averaged 8.1 μg C/m^3 and ranged from 5.9 (before) to 12 μg/m^3 during the two-day event. OM (expressed as 1.8 OC) was generally elevated during the episode, but by only about 30% (see Table 2). Close

TABLE 2
Concentrations of $PM_{2.5}$ mass and major chemical species for 6 pollution episodes

		$PM_{2.5}$, $\mu g/m^3$		Constituent expressed as indicate $\mu g/m^{3,4}$				Constituent, %			
Episode	Interval	TEOM	Reconstructed	(NH4)2SO4	OM	EC	NH4NO3	(NH4)2SO4[4]	OM[4]	EC	NH4NO3
A	Episode Avg.[1]	N/A	55[1], 62[2]	36	16	1.2	1.7	65	29	2.3	3.3
Regional Haze	Episode Range[1]		43–77	28-60	11–22	0.6–2.8	0.6–5.2	54–78	20–34	1.0–5.3	1.1–9.9
	Bkgnd[3]	N/A	24	8.3	12	1.1	0.65	37	51	4.7	1.4
	Bkgnd Range		22–27	5.8–10	11–14	0.6–2.3	0.6–0.7	30–43	32–59	2.6–8.5	1.3–1.5
B	Episode Avg.	57[1], 86[2]	55[1], 82[2]	6.9	54	1.9	2.1	13	81	3	3.2
Canadian Smoke	Episode Range[1]	20–180	20–174	3.7–13	14–161	0.5–3.7	0.25–5.4	3.8–30	65–92	1.4–6.2	1.2–9.0
	Bkgnd[3]	19	18	4.6	12.6	0.5	0.27	25	70	2.8	1.5
	Bkgnd Range	15–17	17–19	2.7–6.2	10–15	0.4–0.5	0.2–0.3	15–36	60–81	2. 6–3.0	1.2–1.7
C	Episode Avg.[1]	49[1], 52[2]	48[1], 52[2]	34	11	1.0	1.0	71	25	2.1	2.3
Regional Haze	Episode Range[1]	24–72	27–65	12.5–49	7.1–15.6	0.4–2.7	0.6–2.2	46–79	19–50	1.1–6.3	1.0–6.1
	Bkgnd[3]	23	23.5	10.4	10.7	1.0	1.4	42	48	4.9	6.1
	Bkgnd Range	12–37	14–33	3.5–16.5	6.4–15	0.5–3.1	0.4–1.2	19–67	25–64	1.9–18	1.7–19
D	Episode Avg.[1]	42[1], 57[2]	39[1], 53[2]	20	16	1.5	1.6	49	42	3.8	4.5
Reg Haze +	Episode Range[1]	36–73	14–68	3.4–42	8–29	0.6–6.4	0.4–5.2	22–71	26–62	1.6–9.3	1.1–16
Local Traffic	Bkgnd[3]	11	13	4.6	7.5	0.7	0.7	34	56	5.6	5
	Bkgnd Range	9.8–12.5	12.9–14	3.2–6	7.1–8	0.7–0.9	0.4–1.1	24–42	50–62	5.0–6.5	3.0–8.2
E	Episode Avg.[1]	35[1], 35[2]	32[1], 35[2]	21	9.1	2.0	1.9	62	27	6	5.4
Regional Haze	Episode Range[1]	8.9–52	11–47	14–28	6.9–15	1.1–3.3	0.5–6.0	47–77	19–34	2.9–11	1.4–13
	Bkgnd[3]	12	14	5.7	6.2	1.0	0.9	44	44	6.4	5.2
	Bkgnd Range	6.5–22	8.1–22	3.5–7.5	3.8–11	0.4–2.5	0.3–2.4	30–55	38–51	3.7–11	2.2–12
F	Episode Avg.[1]	32[1], 32[2]	34[1], 32[2]	7	14	3.3	8.9	22	41	9.6	27
Local Traffic	Episode Range[1]	9.1–87	14.5–83	4.4–1 1	5.2–55	1.2–12	3.6–15	12–31	27–65	4.2–17	7.8–42
	Bkgnd[3]	9.6	14	4.7	4.8	1	3.2	34	35	6.9	23
	Bkgnd Range	7,8–12	13–14	4.2–5.0	4.7–5.1	0.8–1.1	2.5–4.3	29–37	34–37	6.6–7.6	20–30

[1]Average concentration during period of elevation. Background values represent compostlons before and after the episode.
[2]Highest midnight to midnight (24-h) average during episode.
[3]Average before and after episode.
[4]Estimated, see text.

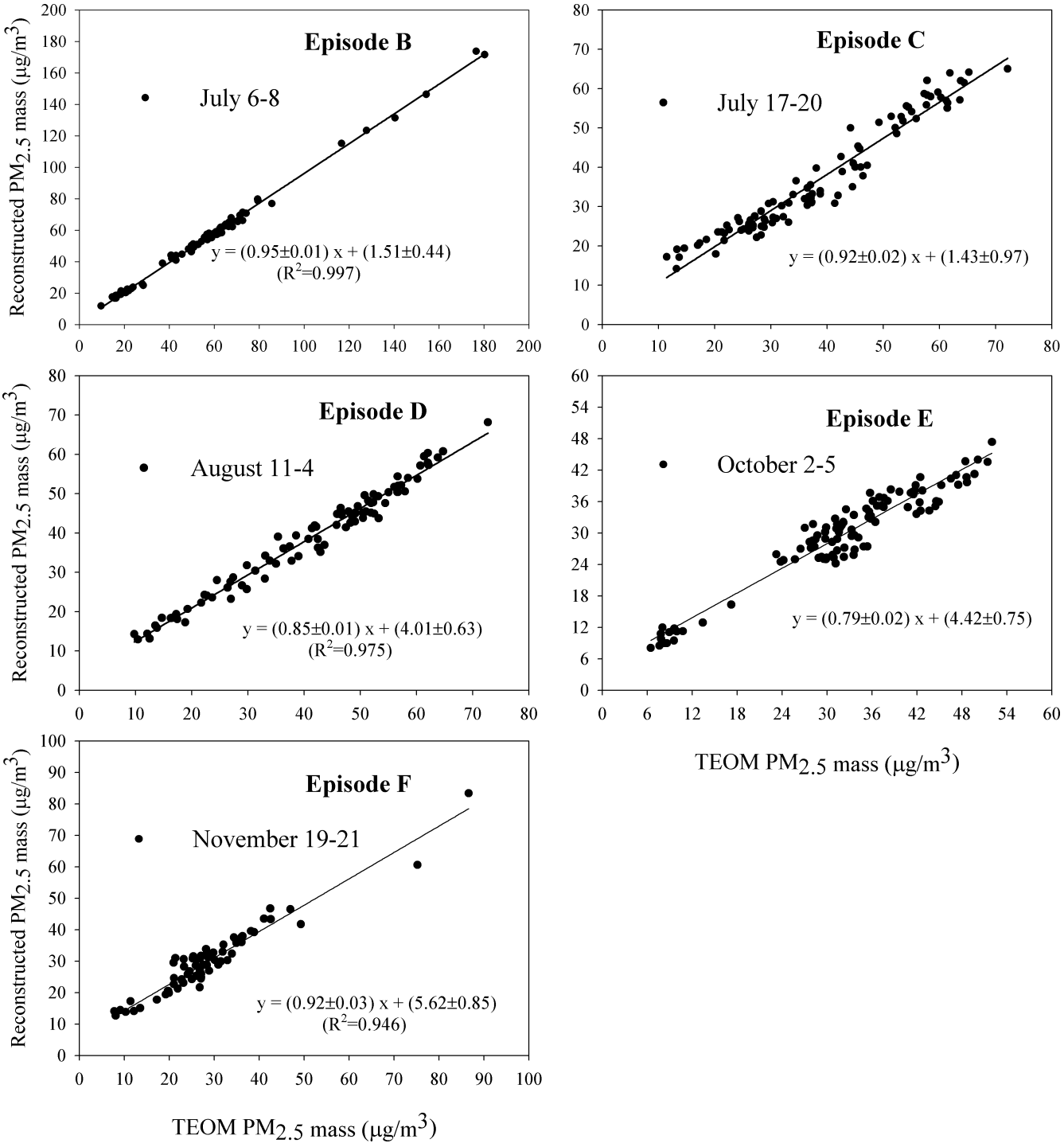

FIG. 3. Scatter plots of TEOM and reconstructed $PM_{2.5}$ mass concentrations for episodes B–F.

inspection of the data reveals that concentrations rose above background starting about 2:00 PM on the 24th, i.e., 2 hours after the peak in ozone. This is consistent with oxidation of organic vapor emissions, emitted earlier by natural and anthropogenic sources. Concentrations of OM declined only slightly during the afternoon and evening of the 24th, with little if any affect of afternoon rush-hour traffic discernable. Concentrations rose again beginning around midnight to a maximum of 19 μg C/m^3 between 3:00 and 6:00 AM on the 25th, coincident with NO_x and slightly later, CO, nitrate, and EC. This is prior to the arrival of air from the Ohio Valley and, owing to the time of day, is attributed to local sources.

TABLE 3
Regression relationship between $PM_{2.5}$, NO_3^-, OC, EC, SO_4^{2-}, and APS (or SMPS)

Episode[1)]	Regression relationship[2)]	R^2
A	**$PM_{2.5} = (0.632 \pm 0.015)\ SO_4^{2-} + (-8.421 \pm 0.699)$**	**0.969**
	$PM_{2.5} = (0.066 \pm 0.007)\ OC + (5.198 \pm 0.326)$	**0.605**
	$PM_{2.5} = (0.003 \pm 0.004)\ EC + (1.073 \pm 0.173)$	0.010
	$PM_{2.5} = (0.008 \pm 0.006)\ NO_3^- + (0.890 \pm 0.289)$	0.027
	$PM_{2.5} = (0.116 \pm 0.007)\ APS + (16.646 \pm 1.817)$	**0.833**
B	**$PM_{2.5} = (0.499 \pm 0.006)\ OC + (-3.006 \pm 0.401)$**	**0.990**
	$PM_{2.5} = (0.018 \pm 0.003)\ NO_3^- + (0.287 \pm 0.173)$	0.409
	$PM_{2.5} = (0.015 \pm 0.003)\ EC + (0.688 \pm 0.164)$	0.359
	$PM_{2.5} = (0.006 \pm 0.007)\ SO_4^{2-} + (4.262 \pm 0.461)$	0.010
	$PM_{2.5} = (0.147 \pm 0.002)\ APS + (12.876 \pm 0.706)$	**0.989**
C	**$PM_{2.5} = (0.662 \pm 0.025)\ SO_4^{2-} + (-9.251 \pm 1.035)$**	**0.880**
	$PM_{2.5} = (0.010 \pm 0.012)\ OC + (6.463 \pm 0.503)$	0.006
	$PM_{2.5} = (-0.005 \pm 0.006)\ EC + (1.266 \pm 0.263)$	0.007
	$PM_{2.5} = (-0.002 \pm 0.004)\ NO_3^- + (0.962 \pm 0.169)$	0.002
	$PM_{2.5} = (0.092 \pm 0.007)\ APS + (20.219 \pm 1.601)$	**0.717**
D	**$PM_{2.5} = (0.403 \pm 0.020)\ SO_4^{2-} + (-2.203 \pm 0.865)$**	**0.830**
	$PM_{2.5} = (0.133 \pm 0.010)\ OC + (3.275 \pm 0.430)$	**0.673**
	$PM_{2.5} = (0.034 \pm 0.006)\ EC + (0.067 \pm 0.245)$	0.298
	$PM_{2.5} = (0.051 \pm 0.005)\ NO_3^- + (0.618 \pm 0.230)$	0.085
	$PM_{2.5} = (0.140 \pm 0.007)\ APS + (17.759 \pm 1.372)$	**0.815**
E	**$PM_{2.5} = (0.377 \pm 0.022)\ SO_4^{2-} + (0.681 \pm 0.740)$**	**0.725**
	$PM_{2.5} = (0.105 \pm 0.013)\ OC + (2.966 \pm 0.418)$	0.389
	$PM_{2.5} = (0.059 \pm 0.007)\ NO_3^- + (-0.554 \pm 0.247)$	0.366
	$PM_{2.5} = (0.035 \pm 0.006)\ EC + (0.368 \pm 0.188)$	0.256
	$PM_{2.5} = (0.093 \pm 0.005)\ APS + (12.684 \pm 1.047)$	**0.807**
F	$PM_{2.5} = (0.049 \pm 0.013)\ SO_4^{2-} + (3.534 \pm 0.440)$	0.246
	$PM_{2.5} = (0.465 \pm 0.027)\ OC + (-2.964 \pm 0.917)$	**0.872**
	$PM_{2.5} = (0.138 \pm 0.009)\ EC + (-1.069 \pm 0.301)$	**0.848**
	$PM_{2.5} = (0.026 \pm 0.027)\ NO_3^- + (6.080 \pm 0.929)$	0.020
	$PM_{2.5} = (0.0004 \pm 0.0000)\ SMPS + (9.151 \pm 2.727)$	**0.653**

[1)]In episode A, $PM_{2.5}$ indicates the reconstructed $PM_{2.5}$. [2)]Units used in the regression analysis are all $\mu g/m^3$ except for APS and SMPS number distributions (cm^{-3}).

Concentrations then declined, until they began increasing at 10:00 AM, coincident with the arrival of Ohio Valley air, and peaked contemporaneously with ozone at 1:00 PM, in part, presumably due to secondary conversion. Concentrations of OM actually declined to nearly background during the period of plume influence discussed above, but peaked again between 9:00 and 11:00 PM along with CO, NO_x, and EC (not shown) as the wind angle inclined from 160 to 220°. This is the direction of the twin traffic tunnel outlets 5 km to the southwest (200°; the MTA bus maintenance yard is also in this direction but is inactive at this time). Tunnel traffic during this period was 60% of the 4:00 to 5:00 PM peak. We have repeatedly observed peaks in traffic associated pollutants (nitrate, CO, EC, OC and ultra fine particles) between 8:00 and 10:00 PM. Increments in OM, NH_4NO_3, and EC during these evening traffic periods totaled 7 $\mu g/m^3$, i.e., ~10% of the corresponding $PM_{2.5R}$.

3.3.2. Episode B (Saturday–Monday, July 6–8, 2002)

Between 6:00 PM July 6 and 1:00 PM on July 8 (Figure 4), the Baltimore Supersite and much of the northeastern United States experienced severe smoke fumigation due to uncontrolled forest fires in Quebec (Pahlow et al. 2005; Park et al. 2004a). Layers with dry air were visible at different heights in IAD radiosonde plots and excellent Lidar coverage of the event facilitated interpretation (Pahlow et al. 2005). During this episode, ambient temperature was lower than the 30-day average with a peak of 28°C on July 6 and a flat peak of 26°C on July 7 caused by attenuation of solar radiation (−35% compared to that on July 5) by the smoke plume. Afterwards the temperature increased to a peak of 34°C on July 8.

$PM_{2.5}$, OC, EC, and CO levels between 6:00 PM July 6 and 0800 July 7 were almost tripled when a coherent layer of smoke at 1300–1500 m experienced subsidence due to high

pressure aloft and was entrained into the mixing layer on July 7 (Pahlow et al. 2005). $PM_{2.5}$, OC, EC, CO, and NOx levels between 6:00 PM July 7 and 8:00 AM July 8 remained high due to calm winds, until a shift in wind direction to southwesterly winds of 3 m/s on 10:00 AM July 8 caused a decline in $PM_{2.5}$, OC, EC, CO, and NO_x. Hourly $PM_{2.5}$ concentrations averaged 56.8 μg/m^3 and the episode maximum (180 μg/m^3) occurred at 12:00 on July 7. OC concentrations were in the range 4.4 to 89 μg C/m^3. In addition, OM (expressed as 1.8*OC), $(NH_4)_2SO_4$, EC, and NH_4NO_3 contributed on average

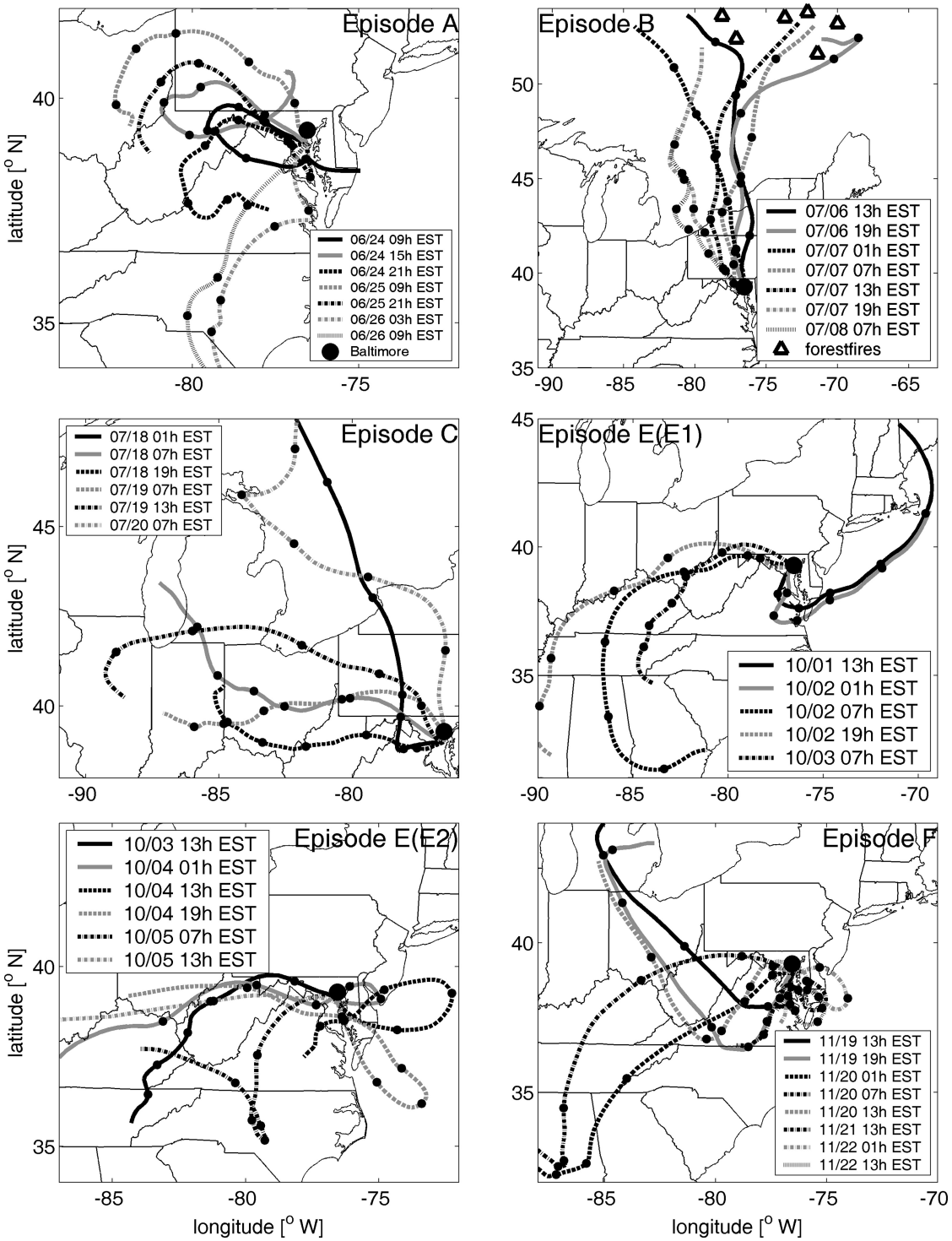

FIG. 4. Air mass backward trajectories arriving at 500 m(MSL) above the Baltimore Supersite for PM episodes A, B, C, E, and F. Point spacing on trajectory curves is 12 hours in each case.

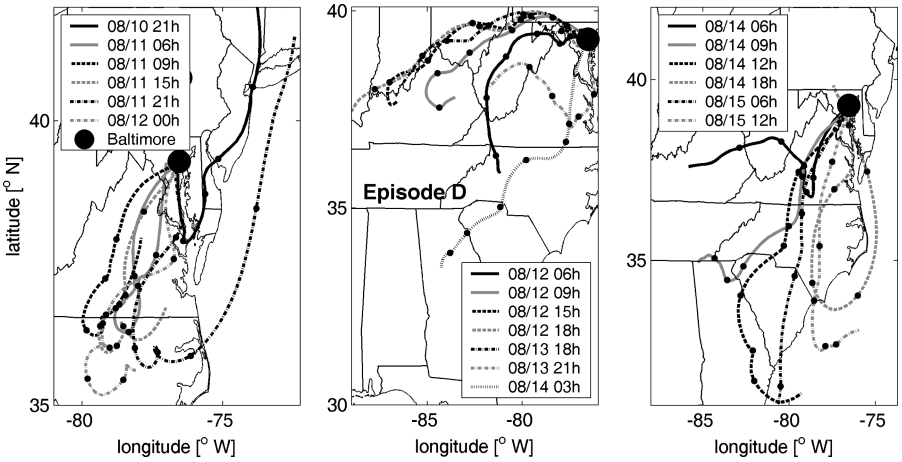

FIG. 4. Air mass backward trajectories arriving at 500 m(MSL) above the Baltimore Supersite for PM episode D. Point spacing on trajectory curves is 12 hours.

79 (60–92%), 14.8 (3.8–36%), 3.0 (1.4–6.3%), and 3.0% (1.2–9.0%) of the $PM_{2.5}$ mass.

NO_x and CO concentrations (Figure 1) showed similar patterns with peaks at 10:00 PM on July 6, 9:00 PM on July 7, and 2:00 AM on July 8, but a strong peak (1.2 ppm) in CO levels occurred around 1:00 PM July 7, suggesting downward mixing of forest fire smoke from aloft. $PM_{2.5}$ was strongly correlated with OC and APS number concentrations (R^2 of 0.990 and 0.989), as shown in Figure 1 and Table 3. Carbon monoxide (CO) was strongly correlated with EC and OC, allowing for the estimation of OC and EC emission factors for boreal forest fires (Park et al. 2004a).

Aged aerosols were, by far, the major components of PM observed during this event as evidenced by the particle number distributions (Figure 2). Interestingly, the size distribution contained modes similar to those observed in episode A (wherein modal diameters were 0.014, 0.21, and 0.58 μm). However, in episode B, the third mode, contained roughly twice the particles (4600 cm^{-3}) as the corresponding mode in episode B, and the second mode was skewed to a larger diameter (0.2 μm from 0.1 μm). The advection of Canadian forest fire smoke into the boundary layer above Baltimore is described by Pahlow et al. (2005).

3.3.3. *Episode C (Thursday–Friday, July 18–19, 2002)*

Episode C began after a stationary front developed on Thursday, July 17th and ended after the passage of a cold front between 2:00 and 5:00 PM on the 19th. The weather was generally hot with maxima of 33–35°C; but inversions were weak and winds, ranging from 1.4 to 4.2 m/s, were not stagnant. Relative humidity ranged from 38–81%, a range sufficient to cause hygroscopic growth. As shown in Figure 1, $PM_{2.5}$ concentrations rose rapidly on the 18th to a maximum of 72 $\mu g/m^3$ while 3-day air mass back trajectories (Figure 4) show that air arriving at Baltimore passed through the lower Ohio Valley and near the Mt. Pleasants power plant near the Maryland panhandle in West Virginia, while local wind directions were, likewise, westerly. Late in the evening, $PM_{2.5}$ concentrations declined, roughly in correlation with the temperature, reaching a low of 38 $\mu g/m^3$ between 4:00 and 6:00 AM on the 18th. Afterwards, $PM_{2.5}$ increased, again, to similar levels between 7:00 AM and 4:00 PM on the 19th, but with air trajectories following a more northerly path from west to east. The passage of the cold front led to strong instantaneous drop in sulfate and $PM_{2.5}$ concentrations at 5:00 PM on the 19th. During this episode, $(NH_4)_2SO_4$, OM (=1.8*OC), EC, and NH_4NO_3 accounted for 71 (46–79%), 25 (19–50%), 2.1 (1.1–6.3%), and 2.3% (1.0–6.1%) of the $PM_{2.5}$ mass on average and, thus, $PM_{2.5}$ mass was clearly dominated by sulfate. Hourly sulfate concentrations averaged 24.9 $\mu g/m^3$, and ranged from 9.1–35.7 $\mu g/m^3$, and, not surprisingly, were strongly correlated with the $PM_{2.5}$ mass concentrations (R^2 of 0.88) as shown in Figure 1 and Table 3. Broad excursions on both the 18th and 19th were correlated with ozone maxima (95 ppb, see Figure 1). On the 18th, sulfate levels increased from the pre-episode background of 6.2 $\mu g/m^3$ to 35 $\mu g/m^3$ at 10:00 PM.

Superimposed on the broad sulfate and $PM_{2.5}$ peaks of the 18th are a series of transients lasting from 2 to 4 hours. These were coincident with local winds from the west (240 to 320°), i.e., along which direction (260°) the nearest power plant lies 60 km away. A 7-h excursion, wherein $PM_{2.5}$ concentrations increased from a low of 16.6 $\mu g/m^3$ at 5:00 AM to 34.3 $\mu g/m^3$ at 2:00 PM, occurred on the 19th. This occurred while winds shifted briefly to the north and then shifted steadily from north through south and back to nearly north again, pausing substantially between 160 and 220°, wherein lie numerous sources in south Baltimore, including the power plants mentioned above.

The dip in sulfate and $PM_{2.5}$ concentrations around 5:00 AM on the19th is coincident with the early morning minimum in the ozone concentration, and thus, both ozone and sulfate in the following peak were driven by photochemistry (Figure 1). In addition, the good correlation of APS number concentrations

with $PM_{2.5}$ mass ($R^2 = 0.717$) indicates that much of the sulfate mass is carried by particles in the far accumulation mode, i.e., at 0.58 μm in the 24- and 1-h (at 2:00 PM) average number size distributions (Figure 2). As described previously, this mode is seen to collect more mass with increasing RH, but with little change in mean diameter (Park et al. 2004b), indicating that smaller particles are growing into this range. As shown in Figure 2, a near accumulation mode at 90 nm is clearly present and prominent at 2:00 PM on the 19th, i.e., in coincidence with the maxima in $PM_{2.5}$ and sulfate on that day, which we, again, attribute to local high-temperature combustion sources, such as the power plants. Three modes were, again, most prominent (i.e., at 0.011, 0.09, and 0.58 μm) and they contained substantially more (31000, 28000, and 1000 cm^{-3}) particles than their corresponding modes in episode A.

3.3.4. *Episode D (Sunday–Wednesday, August 11–14, 2002)*

During Episode D, a strong surface high and upper level ridge developed over the mid-Atlantic region and persisted from August 11 until the evening of August 14. As shown in Figure 4, air arrived at Baltimore along southwesterly trajectories through Virginia and northern North Carolina during the entire day on the 11th. Despite this consistency in transport, sulfate and $PM_{2.5}$ concentrations began to rise after 6:00 AM from pre-event lows (4 and 10 $\mu g/m^3$, respectively) to modest maxima (15.5 and 42.5 $\mu g/m^3$, respectively) between 1:00 and 5:00 PM This occurred in near perfect correlation with increasing temperature and ozone levels which peaked (at 32°C and 84 ppb) under moderate winds (4.2 m/sec). Sulfate and $PM_{2.5}$ concentrations increased most strongly when relatively clean air from the southwesterly trajectories was replaced by air transported from the west over the Ohio Valley on the 12th, which ensued for a period of 2 days (Figure 4). The maximum 24-h average $PM_{2.5}$ concentration (57 $\mu g/m^3$) occurred on the 13th. The episode ended during the afternoon of the 14th, as trajectories shifted more southerly and strong winds (8 to 9 m/s) advected coastal marine air. Between noon and midnight, sulfate and $PM_{2.5}$ concentrations decreased slowly to their pre-episode levels.

During this event, average contributions of major species ($(NH_4)_2SO_4$, 51 (28-71%); OM (=1.8*OC), 41.1 (26–60%); EC 4.1(1.6–9.3%); and NH_4NO_3, 4.0 (1.1–15.6%)) indicate enhanced contributions from OM, EC, and NH_4NO_3 in comparison with episodes A and C.

This episode was further characterized by strong low-level nighttime inversions (i.e., between 6:00 and 9:00 AM on each of the days, including the 11th; see website for IAD sounding), and strong daytime (i.e., between 7:00 AM and 7:00 PM) caps further aloft, again, on each of the days. Local wind speeds were generally weak to moderate (1.4 to 4 m/s), especially in the mornings but exceeded 5 m/s during two periods. Temperatures exceeded the 30-day average (31°C) with maxima in the range 33–37°C between August 11–15. Relative humidity ranged from 35 to 79% during the episode, and thus was often somewhat drier than previous discussed episodes.

Throughout the episode, local wind directions were often between 160 and 220° resulting in a series of short-term excursions superimposed on both background and broadly elevated $PM_{2.5}$ and sulfate levels. The influence of sources in S. Baltimore is, again, evidenced by a series of Sulfate, PM peaks, and the presence of a prominent fresh accumulation mode at 0.09 μm (Figure 2). One such incident occurred between 3:00 PM and 6:00 PM on the 13th and resulted in increments of $\geq$8 and $\geq$10 $\mu g/m^3$ increments in sulfate and $PM_{2.5}$ mass. Another, perhaps, more significant incident probably contributed to the 30 $\mu g/m^3$ increase in PM on the afternoon of the 11th.

The capping inversions favored trapping of air pollutants from local sources close to the ground, e.g., motor vehicle sources. Moreover the morning maxima of NO_x and CO occurred on the 12th, 13th, and 14th (i.e., Monday through Wednesday). The largest was exceeded only in Episode F (see Table 1 and Figure 1). It occurred 6:00 AM on the 13th, during severe stagnation conditions (local wind speed <1.5 m/s) and when winds came from along the direction of the I895/I95 line at 30°. At this time, 1.6-, 6-, and 9-fold excursions in OC, CO, and NO_x, accompanied a 17 $\mu g/m^3$ increase in $PM_{2.5}$ and very high number concentrations (144000 cm^{-3}) of newly emitted particles with a median diameter of approximately 11 nm (Figure 2). Nitrate was also elevated (Harrison et al. 2004).

3.3.5. *Episode E (Wednesday–Saturday October 2–5, 2002)*

This event occurred when a stationary front was established over Baltimore following a frontal reversal. Both local and regional sources contributed to $PM_{2.5}$ excursions. $PM_{2.5}$ concentrations were low (18 $\mu g/m^3$) during the early morning hours of the 1st and began increasing early that evening (~6:00 PM). $PM_{2.5}$ levels fluctuated but remained elevated until the passage of a cold front beginning at 10:00 on Oct 5, which abruptly brought strong (4–8 m/s), dry (RH <50%), west to northwest winds and a reduction in $PM_{2.5}$ to approximately 10 $\mu g/m^3$. During the intervening period the maximum hourly $PM_{2.5}$ was 52 $\mu g/m^3$, and its maximum 24-h average, 42 $\mu g/m^3$, occurred on the 4th, following both a nighttime stagnation and mid-afternoon sulfate event, on the 3rd. Hourly sulfate concentrations ranged from 10 to 21 $\mu g/m^3$ with a mean of 15 $\mu g/m^3$. $PM_{2.5}$ and sulfate were well correlated during the episode (R^2, 0.725; see Table 3 and Figure 1). Average OC concentrations were in the range 4.7–12 $\mu g\ C/m^3$ with a mean of 6.7 $\mu gC/m^3$. Major contributions to $PM_{2.5}$ mass concentrations were: $(NH_4)_2SO_4$, 62.1 (39–77%); OM (1.4*OC), 27.4 (19–43%); EC, 5.0 (2.4–11.2%); and NH_4NO_3, 5.5 (1.3–19%).

The average temperature during the episode was, 25.5°C, with maxima of 30°C on the 2nd and 3rd. On the 1st, 2nd, and 3rd, and again on the 5th, daytime RH was low (<50%), but was >75% during the nights, especially on the evening/morning of the 4th /5th, when it hovered near 91%. Daytime RH remained above 70% on the 4th, apparently buoyed by the passage of

inland air over the Atlantic before arriving in Baltimore (Figure 4, E2). High RH and concomitant deposition of water vapor on particles promotes heterogeneous conversion of SO_2. $PM_{2.5}$ mass and APS number concentrations were well correlated (R^2 of 0.807) as expected for secondary aerosol. Ozone maxima were moderate (60 ppb) and these occurred on each of the afternoons during the episode and both before and after it, as well.

The low $PM_{2.5}$ and sulfate concentrations prior to the onset of the episode occurred as swiftly moving marine air, traveling along the coast from New England, turned inland and arrived in Baltimore from the Southwest (Figure 4, E1). By 7:00 AM on the 2nd, trajectories became much more westerly, passing over the Ohio Valley, through western Maryland, and arriving in Baltimore from the west, at which time sulfate and $PM_{2.5}$ concentrations began increasing to highs of 21 and 42 $\mu g/m^3$, respectively, at 4:00 PM. This flow pattern persisted until 1:00 PM on the 3rd, but sulfate and $PM_{2.5}$ concentrations declined during the prior evening and morning hours. However, as discussed below, the pattern of these sulfate excursions in relation to wind direction suggests that they might have been induced by coherent power plant plumes. Moreover, $PM_{2.5}$ mass is excursions in OM, which appear to be traffic related. Nevertheless, a broad underlying excursion above pre- and post-episode background levels (3 to 5 $\mu g/m^3$ for sulfate) was evident. Low nighttime wind speeds (< 2.4 m/s) and slow circuitous flows accompanied these broader sulfate and $PM_{2.5}$ levels throughout night, until ventilation by high winds (peaking at 7 m/s at 4:30 PM on the 4th) reduced $PM_{2.5}$ to 31 $\mu g/m^3$ and sulfate to 12.5 $\mu g/m^3$. As mentioned above, concentrations of both species declined precipitously with the passage of the cold front at 10:00 AM on the 5th.

The onset of the episode on the 1st corresponded to a shift in the local winds to the direction of the South Baltimore Power plants, to which we attribute elevated sulfate concentrations between 1:00 PM on the 1st and 6:00 AM on the 2nd. Between 11:00 PM on the 1st and 8:00 AM on the 2nd $PM_{2.5}$ mass was affected strongly by OC, as local wind speeds decreased from 2.2 to < 1 m/s and the direction changed to 170 to 230°, which brought air from the MTA bus yard, the two Baltimore Tunnel outlets, and South Baltimore. This OC excursion was well correlated with NO_x and coincident with high CO concentrations and, thus, attributed to vehicular sources (Figure 1). A similar excursion (maximum 11 $\mu g\ C/m^3$) occurred between 6:00 AM and 11:00 AM on the 3rd, when wind speeds again dropped below 1.5 m/s and winds shifted to between 20 and 60°, i.e., the direction of the I-895/I95 line source described above. CO and NO_x (Figure 1) were likewise highly elevated as were EC and nitrate (not shown; Park et al. 2004b). As discussed by Park et al. (2004b), the accompanying high RH ($>80\%$) during this excursion is conducive to the maintenance of particulate nitrate. As shown in Table 3, OC, nitrate, and EC were moderately (R^2 of 0.26–0.39) correlated with $PM_{2.5}$ mass during the episode, largely owing to these excursions.

The particle size spectrum corresponding to the episode's maximum sulfate concentration (5:00 PM, Oct. 3, Figure 2) shows four modes, i.e., 0.014, 0.047, 0.14, and 0.63 μm. The 3^{rd} modal diameter (0.14 μm) is larger and contains less than one-third the particles observed than corresponding modes in episodes A, C, and D, when air at the site was influenced from the South-Baltimore power plants, 15 km away. This larger modal diameter is consistent with a more distant plant (Ondov and Wexler 1998), e.g., the Station H, about 68 km distant. We attribute the 0.014 μm mode to local traffic as discussed above (episode D, spectrum for 6:00 AM) and the 0.63 μm mode to aged aerosol (Ondov and Wexler 1998), which in this case likely contains secondary sulfate derived from emissions in the Ohio Valley. The 47-nm mode may reflect aged nucleation particles formed during high RH conditions the previous evening and arriving in Baltimore after transport over a considerable distance. However, this modal diameter was also observed in the spectrum corresponding to the OC peak at 4:00 on the 2nd, in the traffic-derived episode (F) discussed below.

3.3.6. Episode F (Wednesday–Thursday, November 20–21, 2002)

Between 7:00 PM on the 20th and the end of the episode on the 21st, $PM_{2.5}$ peaked on four occasions, at levels ranging from 32 to 47 $\mu g/m^3$, each along with EC, NO_x and CO. Morning temperatures were seasonable cold, the air was very moist, light winds prevailed, and 24-h average $PM_{2.5}$ concentrations were nearly identical (32 $\mu g/m^3$) on both days, despite a very large excursion on the 20th. In contrast to warm-weather episodes, the major $PM_{2.5}$ constituents were OM ($1.2*OC$), 27–66%; NH_4NO_3, 7.8–43%; $(NH_4)_2SO_4$, 12–31%; and EC, 4.2–17%.

On the 20th a large $PM_{2.5}$ excursion, began developing at 4:00 AM, as temperature and wind speeds declined in the early morning hours, producing a very stable, very weakly mixed, low lying boundary layer. The peak concentration (86.6 $\mu g/m^3$) occurred at 7:00 AM, precisely as wind speeds dropped below 1 m/s and became aligned with the direction of the I895 traffic corridor at 30°. This peak was coincident with large excursions in NO_x (780 ppb). CO (2.8 ppm), and ultra fine particles, and dominated by OC (46 $\mu g\ C/m^3$), EC (11.8 $\mu g/m^3$), and nitrate (5 $\mu g/m^3$), suggesting that the principle source was morning commute traffic. Although not definitive owing to measurement method differences, the OC/EC ratio (3.9) at this time was more consistent with emissions from spark engine vehicles than that for diesels (<2) (Fraser et al. 1998; Kirchstetter et al. 1999). As shown in Figure 2, the particle number distribution at 7:00 AM contained a single prominent feature, i.e., a broad peak at 57 nm with a shoulder on the leading edge at 37 nm, i.e., consistent with those reported by Zhu et al. (2002), at distances of 30 m (65 nm) and 90 m (39 nm) downwind of an LA freeway. A very small shoulder can be seen at approximately 15 nm in the 24-h average spectrum (see in Figure 2). The lack of prominence of this mode can be explained by coagulation, i.e., growth from

this size to 30 or 45 nm is plausible if transport occurred over, e.g., the 7 km length of the I895 corridor.

On the 21st, local winds were again light at 1 to 2 m/s, and almost exclusively from the direction of the I895/I95 roadway line source and a strongly stable, low-lying inversion ensued. The advection of moist air from the Atlantic continued as low temperatures on the 21st induced RH in excess of 90% and fog for most of the day. Interestingly, nitrate concentrations increased steadily from 4.5 $\mu g/m^3$ at 9:00 PM on the 20th, to a maximum of 11.8 $\mu g/m^3$ at 11:00 AM on the 21st, along with increasing RH, fog, and NO_x emissions from morning traffic. These cold, moist conditions efficiently capture nitric acid and suppress ammonium nitrate evaporation (Stelson and Seinfeld 1982). At its peak concentration, nitrate (as ammonium nitrate) comprised 32% of the $PM_{2.5}$ mass. The episode ended around 11:00 AM on the 22nd as a cold front approached with light rain.

4. SUMMARY AND CONCLUSIONS

During the 9.5 months between February 14 and November 30, 2002, the average 30-minute $PM_{2.5}$ mass concentration (16.9 $\mu g/m^3$) exceeded the 15-$\mu g/m^3$ annual standard. Exceedances of the 24-h ambient air quality standard were rare, occurring, at most, on two occasions, one of which encompassed a once-in-a-life-time event caused by transport of smoke from severe Canadian Boreal forest fires in July. Ignoring this, the 9.5-month $PM_{2.5}$ mean was only 15.8 $\mu g/m^3$, arguably, an insignificant deviation from the standard, given measurement uncertainty.

During the study, 29 $PM_{2.5}$ excursions, wherein daily average $PM_{2.5}$ mass concentrations exceeded 30 $\mu g/m^3$, were identified. The 12 worst of these included four, multi-day regional haze episodes in which ammonium sulfate and Organic matter (OM) contributed an estimated 90 to 96% of (episode average) $PM_{2.5}$ mass. Four of these, including the worst (non-smoke) event, occurred in warm summer months or during warm fall conditions of high relative humidity; often following transport regimes from a more source-intense region, and thus when regional SO_2 control would likely be effective. For example, aside from the Canadian Smoke episode, the largest 24-h $PM_{2.5}$ mass concentration occurred after air, previously stagnant over the Ohio Valley, arrived in Baltimore. However, during the preceding day, air flows were circuitous in the local region, and sources in Maryland, southern Pennsylvania, and northern Virginia may have accounted for up to 50% of the observed (2-day episode average) $PM_{2.5}$ concentration. That this is about twice the maximum percentage attributed by Chen et al. (2002) to local sources influencing air in the summers of 1999–2002 at Ft. Meade, MD, 30 km south of Ponca St. and, we believe, warrants further analysis. Analysis of these short-term data further suggest that South Baltimore sources, including the city's two major power plants 15 km away, may frequently induce $PM_{2.5}$ mass increments of $\sim$17 $\mu g/m^3$ at the monitoring site in East Baltimore when the latter is exposed to their plumes.

In late fall and spring, episodes appear to be predominately induced by local automotive traffic. These tend to occur in the early morning while the atmosphere is stable and mixing height is low, but significant excursions in EC, OC, and nitrate often occurred in the late evening. As noted above, the second highest hourly PM excursion (86.6 $\mu g/m^3$) was observed in November in association with cool ($<5^\circ$C), humid ($>90\%$), and calm-to-weak winds from the I895 corridor during the morning rush-hour. During such periods, OM, EC, and ammonium nitrate contributions to $PM_{2.5}$ grew as that of ammonium sulfate declined (e.g., these were respectively, 41%, 9.6, and 27% of the maximum hourly $PM_{2.5}$ mass during the November episode, and ammonium sulfate, only 22%).

REFERENCES

Appel, B. R., Tokiwa, Y., Hsu, J., Kothny, E. L., and Hahn, E. (1985). Visibility as Related to Atmospheric Aerosol Constituents, *Atmos. Environ.* 9:1525–1534.

Chen, A. L.-W., Doddridge, B. G., Dickerson, R. R., Chow, J. C., and Henry, R. C. (2002). Origins of Fine Aerosol Mass in the Baltimore-Washington Corridor: Implications From Observation, Factor Analysis, and Ensemble Air Back Trajectory, *Atmos. Environ.* 36:4541–4554.

Dodd, J. A., Ondov, J. M., Tuncel, G., Dzubay, T. G., and Stevens, R. K. (1991). Multimodal Size Spectra of Submicrometer Particles Bearing Various Elements in Rural Air, *Environ. Sci. Technol.* 25:890–903.

Draxler, R. R., and Rolph, G. D. (2003). *HYSPLIT (Hybrid Single-Particle Lagrangian Integrated Trajectory) model.* http://www.arl.noaa.gov/ready/hysplit4.html, NOAA Air Resources Laboratory, Silver Spring, MD.

Fraser, M. P., Cass, G. R., and Simoneit, B. R. T. (1998). Gas-phase and Particle-Phase Organic Compounds Emitted From Motor Vehicles Traffic in a Los Angeles Roadway Tunnel, *Environ. Sci. Technol.* 32:2051–2060.

Gordon, G. E. (1988). Receptor Models, *Environ. Sci. Technol.* 22:1132–1142.

Harrison, D., Park, S. S., Ondov, J. M., Buckley, T., Kim, S. R., and Jayanty, R. K. M. (2004). Highly-Time Resolved Particulate Nitrate Measurements At The Baltimore Supersite, *Atmos. Environ.* 38:5321–5332.

Harrison, D., and Ondov, J. M. (2006). Highly-Time Resolved Particulate Sulfate Measurements at the Baltimore Supersite, unpublished data, University of Maryland, College Park, MD.

Intergovernmental Panel on Climate Change (IPCC). (1966). *Climate Change 1995: The Science Climate Change*. Cambridge University Press, New York.

Kidwell, C. B., and Ondov, J. M. (2001). Development and Evaluation of a Prototype System for Collecting Sub-Hourly Ambient Aerosol for Chemical Analysis, *Aerosol Science and Technology* 35:596–601.

Kidwell, C. B., and Ondov, J. M. (2004). Elemental Analysis of Sub-Hourly Ambient Aerosol Collections, *Aerosol Science Technol.* 38:1–14.

Kirchstetter, T. W., Harley, R. A., Kreisberg, N. M., Stolzengurg, M. R., and Hering, S. V. (1999). On-Road Measurement of Fine Particle and Nitrogen Oxide Emissions From Light- and Heavy-Duty Motor Vehicles, *Atmos. Environ.* 36:2955–2968.

Lim, H.-J., Turpin, B. J., Edgerton, E., Hering, S. V., Allen, G., Maring, H., and Solomon, P. (2003). Semicontinuous Aerosol Carbon Measurements: Comparison Of Atlanta Supersite Measurements, *J. Geophys. Res.* 108:8419. doi:10.1029/2001JD001214.

Lim, H.-J., and Turpin, B. J. (2002). Origins of Primary and Secondary Organic Aerosol in Atlanta: Results of Time-Resolved Measurements During the Atlanta Supersite Experiment, *Environ. Sci. Technol.* 36:4489–4496.

Malm, W. C., Molenar, J. V., Eldred, R. A., and Sisler, J. F. (1996). Examining the Relationship Among Atmospheric Aerosols and Light Scattering and Extinction in the Grand Canyon Area, *J. Geophys. Res.* 101:19251–19265.

National Research Council (NRC). (1996). Aerosol Radiative Forcing And Climate Change,, National Academy Press, Washington DC, pp. 161.

Oktem, B., Tolocka, M. P., and Johnston, M. V. (2004) On-Line Analysis of Organic Components in Fine and Ultra Fine Particles By Photoionization Aerosol Mass Spectrometry, *Anal. Chem.* 76:253–261.

Ondov, J. M., and Wexler, A. S. (1998). Where do Particulate Toxins Residue? An Improved Paradigm for the Structure and Dynamics of the Urban Mid-Atlantic Aerosol, *Environ. Sci. Technol.* 32:2547–2555.

Pahlow, M., Kleissl, J., Parlange, M. B., Ondov, J. M., and Harrison, D. (2005). Atmospheric Boundary Layer Structure as Observed During a Haze Event Due to Forest Fire Smoke, *Boundary-Layer Meteorol.* 114:53–70.

Park, S. S., Harrison, D., Pancras, J. P., and Ondov, J. M. (2005) Highly Time-Resolved Organic and Elemental Carbon Measurements at the Baltimore Supersite in 2002, *J. Geophys. Res. 110*, D7 2004JD004610 D07S06

Peters, A., Dockery, D. W., Muller, J. E., and Mittleman, M. A. (2001). Increased Particle Air Pollution And Triggering Of Myocardial Infraction, *Circulation* 103:2810–2815.

Pope, C. A. I., (2000) Review: Epidemiological Basis for Particulate Air Pollution Health Standards, *Aerosol Sci. Technol.* 32:4–14.

Rheingrover, S. W., and Gordon, G. E. (1988). Wind-Trajectory Method for Determining Compositions of Particles from Major Air Pollution Sources, *Aerosol Sci. Technol.* 8:29–61.

Solomon, P. A., Chameides, W., Weber, R. W., Middlebrook, A., Kiang, C. S., Russell, A. G., Butler, A., Turpin, B., Mikel, D., Scheffe, R., Cowling, E., Edgerton, E., St. John, J., Jansen, J., McMurry, P., Hering, S., and Bahadori, T. (2003). An Overview of the 1999 Atlanta Supersites Project.? *JGR ? Atmospheres, Special Issue for the Atlanta Supersites Project*, 108(D7), 8428 doi:10.1029/2001JD001458

Stelson, A. W., and Seinfeld, J. H. (1982). Relative Humidity and Temperature Dependence of the Ammonium Nitrate Dissociation Constant, *Atmos. Environ.* 16:983–992.

Stolzenburg, M. R., and Hering, S. V. (2000). Method For The Automated Measurement of fine Particle Nitrate in the Atmosphere, *Environ. Sci. Technol.* 34:907–914.

Turpin, B. J., and Lim, H.-J. (2001). Species Contributions To $PM_{2.5}$ Mass Concentrations: Revisiting Common Assumptions For Estimating Organic Mass, *Aerosol Sci. Technol.* 35:602–610.

Watson, J. G., and Chow, J. C. (2002). A Wintertime $PM_{2.5}$ Episode at the Fresno, CA, Supersite, *Atmos. Environ.* 36:465–475.

Weber, R. J. et al. (2003a). Intercomparison of Near Real-Time Monitors of $PM_{2.5}$ Nitrate and Sulfate at the EPA Atlanta Supersite, *J. Geophys. Res.* 108:8421. doi:10.1029/2001JD001220.

Weber R. J. et al. (2003b). Short-Term Temporal Variation In $PM_{2.5}$ Mass And Chemical Composition During The Atlanta Supersite Experiment, *J. Air Waste Mange. Assoc* 53:84–91.

Zhang, K. M., Wexler, A. S., Zhu, Y., Hinds, W., and Sioutas, C. (2004). Evolution of Number Distributions Near Roadways, Presented at the EPA Supersites principle investigator's workshop, Las Vegas, February 25–26.

Zhu, Y., Hinds, W. C., Kim, S., Shen, S., and Sioutas, C. (2002). Study of Ultra Fine Particles Near A Major Highway With Heavy-Duty Diesel Traffic, *Atmos. Environ.* 36:4323–4335.